

## Light Propagation in Strongly Scattering, Random Colloidal Films: The Role of the Packing Geometry

X. T. Peng and A. D. Dinsmore\*

*Department of Physics, Univ. of Massachusetts Amherst, Massachusetts 01003, USA*

(Received 24 February 2007; revised manuscript received 4 May 2007; published 2 October 2007)

We study the propagation of light through randomly packed films of micron-sized spheres. Dried films consist of strongly scattering core-shell particles mixed with polymer spheres, which are then dissolved to tune the number of contacts,  $Z$ , among the remaining scatterers. The transport mean free path  $l^*$  is measured from the width of the coherent backscattering cone;  $l^* = 2.1 \mu\text{m}$  when  $Z \sim 4-5$ , but increases twofold (scattering weakens) in a film with  $Z \sim 9-10$ . The results contradict the standard diffusive transport model, but are explained by accounting for optical coupling of contacting spheres.

DOI: [10.1103/PhysRevLett.99.143902](https://doi.org/10.1103/PhysRevLett.99.143902)

PACS numbers: 42.25.Dd, 42.25.Bs, 47.57.J-

The past decade has seen great strides toward fabrication of materials to control the propagation and emission of light and the appearance of materials with a spatially varying index of refraction. Ordered arrays of wavelength-sized spheres (“photonic crystals”) allow considerable control of the density of propagating wave states, in part owing to Bragg-like reflections from the crystal planes [1]. Random arrangements of particles also lead to fascinating problems in light propagation, such as diffusion of light, which leads to coherent backscattering [2] and, in the limit of strong scattering, to strong localization [3–6]. Random, opaque media are typically characterized by the transport mean free path for photons (or random-walk step length),  $l^*$  [7,8]. Effective medium theories for scalar waves predict that, in random systems, the optimal packing fraction to minimize  $l^*$  or maximize scattering is  $\phi \sim 0.2-0.5$  [9–11]. The standard diffusive transport model for  $l^*$  [8,12–15] incorporates structural correlations among scatterers and can lead to similar predictions, which agree with experiments in the regime where  $l^* \geq 10\lambda$  [14–19]. In the strong-scattering regime, however, where  $l^*$  is comparable to the wavelength ( $\lambda$ ) or sphere diameter ( $d$ ), experiments are still needed to test the diffusive transport model and to understand more clearly the role of the structure. Here, we report on experimental measurements of the propagation of light through randomly packed spherical particles with  $d \sim 1 \mu\text{m}$  and  $\lambda = 1.06 \mu\text{m}$ . The coherent backscattering of light was used to measure  $l^*$ , which was as small as  $2.1 \mu\text{m}$ . We show that the average coordination number,  $Z$ , plays an important role in determining the optical properties. In particular, reducing  $Z$  to  $\sim 4$  by dissolving a controlled fraction of spheres decreased  $l^*$  by a factor of 2.2 compared to close-packed samples. In contrast to our data, the diffusing-wave transport theory predicts that  $l^*$  decreases monotonically as  $Z$  is increased. We describe a correction to this theory, which approximately accounts for optical coupling of neighboring spheres and with which we obtain good agreement with our experimental data. The results should be useful in fabricating samples with small

$l^*$  to enhance opacity of paints or cosmetics, to attain strong localization of light [3–6], and to understand in general the role of coordination number in wave propagation.

Samples were prepared from binary aqueous suspensions of colloidal spheres. Poly(methylmethacrylate) spheres (PMMA; Bangs Labs) served as sacrificial particles; they were dissolved after the film was made. The scatterers were polystyrene (PS) spheres, which were coated with a  $\sim 80\text{-nm}$ -thick layer of ZnS in order to enhance their scattering cross section: the PS core and ZnS shell have  $n = 1.59$  and  $2.0$ , respectively [20] (inset of Fig. 1). The ZnS-PS particles were synthesized using a sonochemical technique [20,21]. Controlled volumes of the aqueous suspensions of PMMA and ZnS-PS spheres were mixed to set the number ratio  $f$  of ZnS-PS spheres to the total number of spheres. The value of  $f$  has a systematic uncertainty of  $\sim 4\%$ . Films of thickness  $100-150 \mu\text{m}$  were

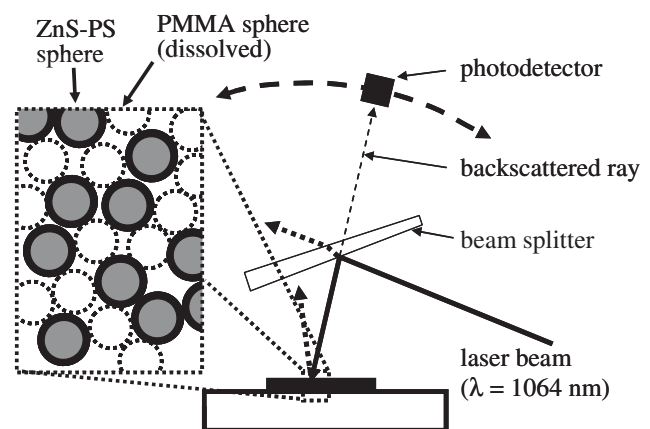


FIG. 1. Schematic of coherent backscattering setup. A beam splitter allows sample illumination and detection of the backscattered light by the Si photodiode. The inset schematically shows the samples studied here. Dissolving the PMMA spheres allows us to tune  $Z$ , the coordination of the remaining ZnS-PS scatterers.

prepared by drying the microspheres from suspension onto a glass plate, using a machined Teflon ring to control the shape of the meniscus and leave a flat film [21].

To strengthen some of the films for later handling, an aqueous solution (400  $\mu\text{L}$ ; refractive index 1.41) of 100:100:7:2 (by weight) water, acrylamide,  $N$ ,  $N'$ -methylenebisacrylamide, and diethoxyacetophenone was placed atop the particle films before they had completely dried. The solution was then rapidly photopolymerized into a transparent polyacrylamide hydrogel under ultraviolet illumination, and the film was detached from the glass. The hydrogel provided a supporting layer, but did not penetrate to the illuminated surface at high concentration.

To vary the coordination number,  $Z$ , of the ZnS-PS spheres, we dissolved the PMMA spheres within the dried films. Dried films were immersed in acetone for 20 min, then in fresh acetone for 10 min, and then dried. In control samples containing only PMMA spheres, the PMMA dissolved in a few minutes. In samples containing only ZnS-PS spheres or polyacrylamide hydrogel, the particles and gel did not dissolve even after 2 hrs. Samples were inspected using a scanning electron microscope (SEM) before and after acetone treatment; these images showed that the remaining ZnS-PS spheres were still spherical and that the film remained intact when  $f \geq 0.3$  [21].

The transport mean free path  $l^*$  of the films was measured from the coherent backscattering effect [2,12,14,22–26]. Owing to constructive interference of light propagating forward and backward along identical paths through the sample, the intensity has a peak in the backscattering direction and decays with a characteristic angular width that is related to  $l^*$  (see text below) [23,26]. A 50-mW diode laser with  $\lambda = 1.064 \mu\text{m}$  was used as a source, and a set of gold mirrors, lenses, and apertures guided the vertically polarized laser beam to an uncoated  $3^\circ$  wedged beam splitter (CVI Laser, LW-3-2050-C) and then to the film. The illuminated region was 2–3 mm in diameter. The backscattered light was collected by a silicon photodiode mounted to a goniometer to scan the angle,  $\theta$  (Fig. 1). The angular width of the detection was 3 mrad and the goniometer was scanned in increments of 3.5 mrad. For the data reported here, the effect of the finite angular resolution on the measured  $l^*$  was small, approximately 1%. Data were obtained without a linear polarizer in front of the detector so as to maximize the intensity; control measurements with an analyzer resulted in values of  $l^*$  that were within  $8 \pm 4\%$  of the values without an analyzer. A chopper and lock-in amplifier were used to acquire the data and remove extraneous light. Stray and backscattered beams were blocked to prevent backscattering into the detector. The direction normal to the film's surface was set  $\sim 10^\circ$  away from the incident direction to separate the specular-reflection peak from the coherent-backscattering peak [12]. A small motor (vibration amplitude = 2–3 mm) was used to oscillate the

angle between the film and the incident beam by  $\sim 2^\circ$  to average over interference speckles [27,28]. Without this oscillation, the speckle pattern created sharp spikes in the intensity profile.

Figure 2 shows the intensity profile measured from films of ZnS-PS and PMMA spheres, with diameters of 1.00 and 1.08  $\mu\text{m}$ , respectively. (Note that the ZnS-PS diameter refers to the PS core diameter.) The plot inset shows the measured  $I(\theta)$ , which exhibits a peak at the direct backscattering angle and an exponential decay. We fit the data to  $I(\theta) = I_b + A \exp[-|\theta - \theta_0|/\Delta\theta]$ , where  $I_b$  is the reflected background intensity,  $\theta_0$  is an offset in the backscattering angle, and  $\Delta\theta$  is angular width of the peak. The value of  $l^*$  is then calculated from the width using  $W = 0.7\lambda/(2\pi l^*)$  [23,26], where  $W = 2\Delta\theta \ln 2$  is the full width at half maximum of  $I(\theta)$ . The inset of Fig. 2 shows the fitted  $I(\theta)$  convolved with the angular resolution of the experiment. To further demonstrate the quality of these fits, Fig. 2 shows the data in a rescaled form,  $\ln\{[I(\theta) - I_b]/A\}$ . We found that the peak-to-background ratio  $(I_b + A)/I_b$  in our samples ranges between 1.3 and 1.4, as expected for unpolarized-light detection [26,29,30]. For comparison, we also measured  $l^*$  by transmittance through a sample, which scales with  $L/l^*$  [18,31–34]. For binary films of PMMA and PS ( $f = 0.5$ , and diameters  $d = 1.48 \mu\text{m}$  and  $1.58 \mu\text{m}$ ), we obtained  $l^* = 3.8 \pm 0.2 \mu\text{m}$ , which agrees with the result of the coherent backscattering for the same sample ( $3.8 \pm 0.12 \mu\text{m}$ ). All of the  $l^*$  measurements were repeated on multiple spots on given films as well as on different films with the same composition.

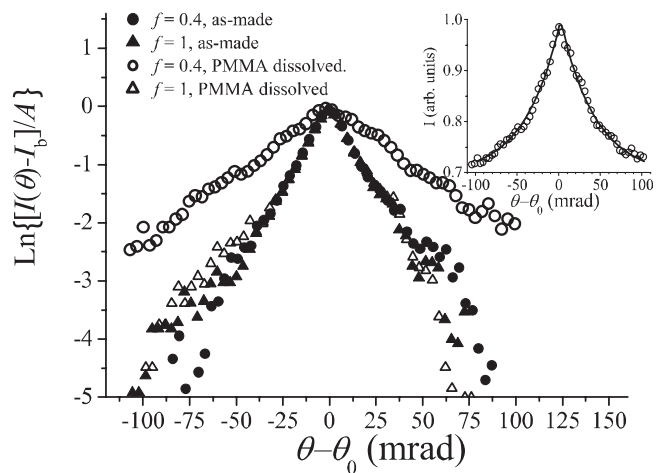


FIG. 2. Backscattered intensity from films of ZnS-PS and PMMA spheres. The solid symbols show results of the binary films with  $f = 0.40$  and 1. The open symbols show the same samples after the PMMA spheres were dissolved. Data are plotted as  $\ln\{[I(\theta) - I_b]/A\}$  vs  $(\theta - \theta_0)$  so that the slope is proportional to  $l^*$ . (Inset)  $I(\theta)$  for the sample with  $f = 0.40$  after the PMMA were dissolved. The curve shows the result of a fit convolved with the angular resolution.

Figure 3(a) shows the measured  $l^*$  for binary films without the polyacrylamide hydrogel. We find an overall trend of decreasing  $l^*$  as  $f$  is increased (though in many experiments, we found a local minimum near  $f = 0.5$ ). This overall trend is explained by the larger scattering cross section of the ZnS-PS spheres, which leads to a shorter  $l^*$ . In similar binary films with the polyacrylamide hydrogel [Fig. 3(b), solid circles], we found a slightly larger  $l^*$ . We attribute this trend to a partial filling of the interstices by the added hydrogel, which would reduce the refractive-index contrast and increase  $l^*$ .

In Fig. 3(b), the solid and open circles show the same films before and after the PMMA spheres were dissolved. Dissolving the PMMA spheres clearly decreased  $l^*$  (i.e., enhanced scattering). The change was substantial: when  $f = 0.4$ ,  $l^*$  decreased from  $4.70 \pm 0.22 \mu\text{m}$  to  $2.07 \pm 0.15 \mu\text{m}$ . As expected, we found that the sample with  $f = 1.0$  (no PMMA) showed no significant change after the acetone wash. The most striking result, however, is that scattering is relatively weak in the sample with the highest concentration of ZnS-PS scatterers. Instead, we found the

local minimum  $l^*$  (or strongest scattering) when  $f \sim 0.4$ . Samples with  $f \leq 0.2$  collapsed after dissolving the PMMA spheres because the number of remaining contacts could not support the film. From analysis of confocal microscopy images of similarly concentrated particle suspensions, we found that this optimal  $f = 0.4$  corresponds to coordination number  $Z \sim 4$  [21].

For comparison to our data, we computed  $l^*$  using a standard model of diffusive transport of electromagnetic waves in random media [8,12–15,17,35]:  $\frac{1}{l^*} = \frac{\pi}{k_0} \times \int_0^{2k_0} \frac{\phi_0 f}{(\pi/6)d^3} \frac{d\sigma}{d\Omega} S(q) q^3 dq$  where the scattering wave vector  $q = 2k_0 \sin\theta/2$ ,  $k_0 = 2\pi/\lambda$ , and  $\phi_0$  is the volume fraction of particles in the dried film (PMMA and ZnS-PS together). The product  $\phi_0 f$  is the volume fraction of the remaining ZnS-PS scatterers after dissolving the PMMA,  $S(q)$  is the structure factor of the ZnS-PS scatterers, and  $d\sigma/d\Omega$  is the differential scattering cross section of a single ZnS-PS scatterer in the surrounding air. The above approach treats the particles as isolated scatterers (to obtain  $d\sigma/d\Omega$ ); interference among the waves scattered from other particles is accounted for by  $S(q)$ . We obtained  $S(q)$  for a single-component hard-sphere fluid in equilibrium with the “rational function approximation” within liquid structure theory (from [36]), using the Carnahan-Starling equation of state for hard spheres and assuming  $\phi_0 = 0.64$ . To account for the changing  $f$ , we assume that the dissolved PMMA particles were randomly distributed in space and that the ZnS-PS spheres remain fixed. Consequently, the radial distribution function,  $g(r)$ , of the ZnS-PS spheres is independent of  $f$ . (There are fewer pairs of spheres with a given separation, but this factor is removed when normalizing by the average density of the sample.) Since  $S(q) = 1 + \frac{\phi_0 f}{(\pi/6)d^3} \int d\vec{r} e^{i\vec{k}\cdot\vec{r}} [g(r) - 1]$ , a fixed  $g(r)$  means that  $[S(q) - 1]/f$  equals a constant that is calculated from the single-component case,  $f = 1$  [15]. The differential scattering cross section  $d\sigma/d\Omega$  of ZnS-PS core-shell spheres with a shell thickness of 80 nm was calculated with Mie theory using a numerical routine [37,38]. As shown by the solid curve in Fig. 3(b), this model predicts that  $l^*$  decreases monotonically with increasing  $f$ , which contradicts our experimental results. Earlier measurements of  $l^*$  in suspensions [14–19] showed quantitative agreement with this model when the appropriate  $S(q)$  was used. In the present experiments, however, the scatterers are in contact with one another. We propose that under these conditions,  $d\sigma/d\Omega$  should not be derived from the isolated-particle result because, even near a Mie resonance, the electric field extends to the neighboring spheres.

As a correction, therefore, we use a modified cross section that corresponds to an isolated ZnS-PS sphere in a background with effective refractive index,  $n_{\text{eff}}$ . The value of  $n_{\text{eff}}$  accounts for the coupling of neighboring spheres over a distance  $R$ . The length  $R$  should scale with  $\lambda/n_b$ , which sets the penetration depth of an evanes-

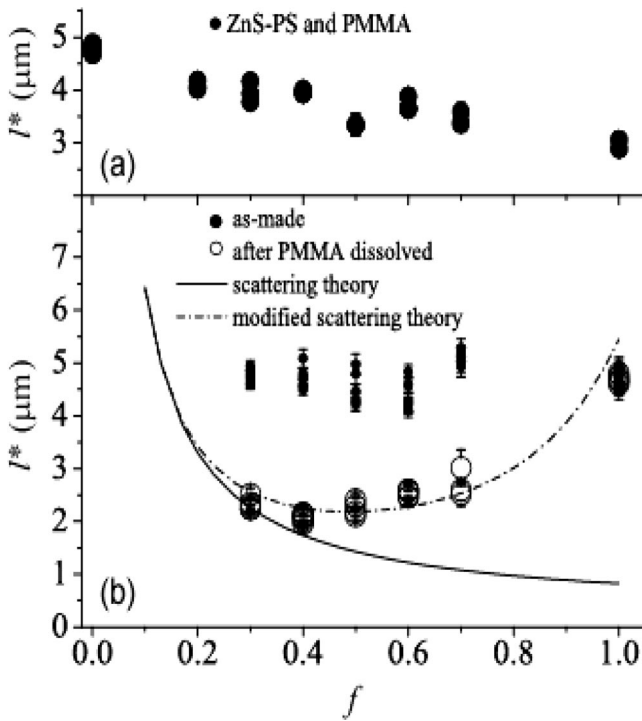


FIG. 3. Measured  $l^*$  vs the number fraction of strongly scattering ZnS-PS spheres,  $f$  (a) Transport mean free path,  $l^*$ , measured in mixtures of ZnS-PS spheres (1000 nm-PS-core-80 nm-ZnS-shell) and PMMA spheres (1080 nm diameter). (b) Measured  $l^*$  in mixtures of ZnS-PS and PMMA spheres with cross-linking polymer added (●). The open circles (○) show  $l^*$  of the same films after the PMMA spheres were dissolved, leaving only the ZnS-PS spheres. The solid curve shows the prediction of the standard scattering theory, while the dashed curve shows the prediction of the modified theory discussed in the text.

cent wave at a flat dielectric interface. We estimated  $n_{\text{eff}}$  from the volume-averaged refractive index within a spherical region of radius  $R$  surrounding a typical scatterer. The values of  $l^*$  were then calculated using the modified cross section. We found reasonable agreement with the data with the empirical choice  $R = (n_s/n_b)\lambda/2$ , where  $n_s$  and  $n_b$  are the refractive indices of the sphere and background [21]. These results agree closely with our experimental data [dashed curve, Fig. 3(b)]. The agreement of this model with the data shows that the reduction of scattering at large  $f$  arises from the loss of refractive-index contrast between an individual scatterer and its many nearby neighbors (i.e., the background). The correction incorporates this effect in a quantitatively reasonable way. To check the general utility of our approach, we applied the same correction to published experiments done with aqueous suspensions of 0.46- $\mu\text{m}$ -diameter PS spheres [14]; because the spheres were not close packed and the refractive-index contrast between spheres and solvent was modest, this correction had a very small effect over the range of  $\phi$  studied.

Our experiments show clearly that the transport mean free path,  $l^*$ , of a close-packed random film of monodisperse spheres increases as  $f$  changes from 0.4 to 1. The value of  $l^*$  exhibits a local minimum when the spheres are packed with a reduced mean coordination number ( $Z \sim 4$ ). The results are quantitatively explained by a loss of refractive-index contrast between an individual scatterer and the background when  $Z$  is too large. Our maximally scattering structure has  $\phi \sim 0.26$ , which is consistent with effective medium theories for scalar waves with large index mismatch [9–11]. From a practical point of view, this method of using sacrificial particles has the additional advantage of providing a solid matrix in a low-index (air) background, since the remaining scatterers remain in contact even at low  $Z$  and  $\phi$ . Hence, this approach might find application in designing coatings or other amorphous materials with strongly modulated density of states.

We thank N. Menon for valuable discussions and Qijun Xiao and Mark Tuominen for assistance with the electron microscopy. We gratefully acknowledge support from the NSF-supported Materials Research Science and Engineering Center on Polymers (No. DME-0213695). A. D. D. thanks the Research Corporation for financial support.

---

\*dinsmore@physics.umass.edu

- [1] J. D. Joannopoulos, R. D. Meade, and J. N. Winn, *Photonic Crystals* (Princeton Univ. Press, Princeton, NJ, 1995).
- [2] P. E. Wolf and G. Maret, Phys. Rev. Lett. **55**, 2696 (1985).
- [3] S. John, in *Scattering and Localization of Classical Waves in Random Media*, edited by P. Sheng (World Scientific, Singapore, 1990).
- [4] D. S. Wiersma *et al.*, Nature (London) **390**, 671 (1997).
- [5] D. S. Wiersma *et al.*, Nature (London) **398**, 207 (1999).
- [6] A. A. Chabanov and A. Z. Genack, Phys. Rev. Lett. **87**, 153901 (2001).
- [7] A. Ishimaru, Proc. IEEE **65**, 1030 (1977).
- [8] D. J. Pine *et al.*, in *Scattering and Localization of Classical Waves in Random Media*, edited by P. Sheng (World Scientific, Singapore, 1990).
- [9] Z.-Q. Zhang and P. Sheng, in *Scattering and Localization of Classical Waves in Random Media*, edited by P. Sheng (World Scientific, Singapore, 1990).
- [10] K. Busch and C. M. Soukoulis, Phys. Rev. Lett. **75**, 3442 (1995).
- [11] K. Busch and C. M. Soukoulis, Physica B (Amsterdam) **296**, 56 (2001).
- [12] P. E. Wolf *et al.*, J. Phys. (France) **49**, 63 (1988).
- [13] F. C. Mackintosh and S. John, Phys. Rev. B **40**, 2383 (1989).
- [14] S. Fraden and G. Maret, Phys. Rev. Lett. **65**, 512 (1990).
- [15] P. M. Saulnier, M. P. Zinkin, and G. H. Watson, Phys. Rev. B **42**, 2621 (1990).
- [16] P. D. Kaplan, A. G. Yodh, and D. J. Pine, Phys. Rev. Lett. **68**, 393 (1992).
- [17] L. F. Rojas-Ochoa *et al.*, Phys. Rev. E **65**, 051403 (2002).
- [18] L. F. Rojas-Ochoa *et al.*, Phys. Rev. Lett. **93**, 073903 (2004).
- [19] K. C. Wu *et al.*, J. Appl. Phys. **98**, 024902 (2005).
- [20] M. L. Breen *et al.*, Langmuir **17**, 903 (2001).
- [21] See EPAPS Document No. E-PRLTAO-99-003740 for supplementary material. For more information on EPAPS, see <http://www.aip.org/pubservs/epaps.html>.
- [22] E. Akkermans, P. E. Wolf, and R. Maynard, Phys. Rev. Lett. **56**, 1471 (1986).
- [23] M. B. van der Mark, M. P. van Albada, and A. Lagendijk, Phys. Rev. B **37**, 3575 (1988).
- [24] S. Mitani, K. Sakai, and K. Takagi, Jpn. J. Appl. Phys. **39**, 146 (2000).
- [25] S. Murai *et al.*, Jpn. J. Appl. Phys. **43**, 5359 (2004).
- [26] R. Sapienza *et al.*, Phys. Rev. Lett. **92**, 033903 (2004).
- [27] S. Etamad, R. Thompson, and M. J. Andrejco, Phys. Rev. Lett. **57**, 575 (1986).
- [28] J. H. Li and A. Z. Genack, Phys. Rev. E **49**, 4530 (1994).
- [29] M. P. van Albada and A. Lagendijk, Phys. Rev. Lett. **55**, 2692 (1985).
- [30] J. Huang *et al.*, Phys. Rev. Lett. **86**, 4815 (2001).
- [31] D. J. Pine *et al.*, J. Phys. (Les Ulis, Fr.) **51**, 2101 (1990).
- [32] P. D. Kaplan *et al.*, Appl. Opt. **32**, 3828 (1993).
- [33] J. H. Li *et al.*, Europhys. Lett. **22**, 675 (1993).
- [34] P. D. Kaplan *et al.*, Phys. Rev. E **50**, 4827 (1994).
- [35] G. Maret and P. E. Wolf, Z. Phys. B **65**, 409 (1987).
- [36] M. L. de Haro and M. Robles, J. Phys. Condens. Matter **16**, S2089 (2004).
- [37] C. F. Bohren and D. R. Huffman, *Absorption and Scattering of Light by Small Particles* (Wiley, New York, 1998).
- [38] A. L. Aden and M. Kerker, J. Appl. Phys. **22**, 1242 (1951).